ChemComm

Accepted Manuscript

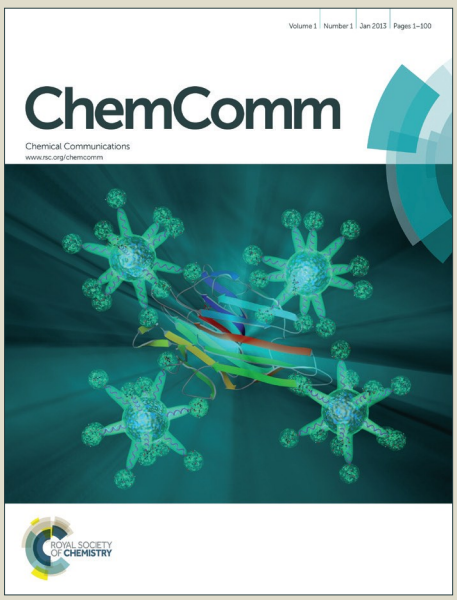

ROYAL SOCIETY OF CHEMISTRY

www.rsc.org/chemcomm

Journal Name

RSCPublishing

COMMUNICATION

Branched dimerization of Tat peptide improves permeability to HeLa and hippocampal neuronal cells

Cite this: DOI: 10.1039/xoxxoooooox

I. Abrrey Monreal,[1] Qian Liu,[2] Katherine Tyson,[3] Tyler Bland,[3] Doralyn S. Dalisay,[4] Erin V. Adams,[1] Gary A. Wayman,[3] Hector C. Aguilar,[2] and Jonel P. Saludes[1]*

Received ooth January 2012,
Accepted ooth January 2012

DOI: 10.1039/xoxxoooooox

www.rsc.org/

A dimeric branched peptide TATp-D designed as an analogue of the HIV-Tat protein transduction domain (TATp), a prototypical cell penetrating peptide (CPP), demonstrates significantly enhanced cell uptake at 0.25 to 2.5 μM. Live cell confocal laser scanning microscopy revealed that multivalency dramatically improved the permeation potency of TATp-D to HeLa and primary hippocampal neuronal cells. The observed enhanced ability of TATp-D to translocate through the membrane is highlighted by a non-linear dependence on concentration, exhibiting the greatest uptake at sub-micromolar concentrations as compared to TATp. Multimerization via bis-Fmoc Lysine offered a synthetically straightforward method to investigate the effects of multivalent CPPs while offering orthogonal handles for cargo attachment, increasing the utility of CPPs at significantly lower concentrations.

The plasma membrane is impermeable to a large number of compounds, including bioactive molecules such as peptides, proteins and oligonucleotides, serving as an efficient and necessary barrier to protect cells. However, in diseased states and in conditions where it is desirable to deliver therapeutics intracellularly where ~90% of druggable targets are located, an efficient non-membranolytic, non-viral delivery vector is highly desirable.[1, 2] The use of short peptide sequences as membrane permeable agents, hereinafter called cell penetrating peptides (CPPs), stems from the discovery of the protein transduction domain in HIV-1 Tat,[3] where a short, cationic, arginine-rich sequence TATp 48-60 (GRKKRRQRRRPPQ, **4**, Figure 1) was found to be responsible for its translocation property.[1] Since then, a large array of protein-derived and rationally-designed guanidinium-containing CPPs have been defined including octaarginine (**2**), penetratin (**3**), pVEC, and VP22 among others.[4, 5] TATp and related protein-derived CPPs show great promise as delivery agents but face the limitations of poor translocation efficiency,[6] lack of target specificity, cytotoxicity, and penurious biostability.[4]

It is interesting to note, however, that multimers and dendrimers of CPPs have shown higher cellular uptake compared to their parent monomers.[7-9] Branched or multivalent designs often leads to increased uptake, which in turn increases efficacy at much lower concentrations. For instance, co-administration of tetramers of **3** and **4** increased transduction efficiency into mesenchymal stem cells by three orders of magnitude compared to the monomer.[8] Further, CPP multimers can be designed to be proteolysis resistant compared to their linear precursors[10] and are generally not cytotoxic at therapeutic concentrations.[11] We sought to utilize a solid phase peptide synthesis method for preparing multimeric CPPs and investigate the effects of multivalency on cell membrane permeability. We hypothesized that simple dimerization through a *C*-terminal Lys residue to keep the main peptide sequence unaltered will lead to increased cell uptake efficiency, hence requiring less amount of peptide to effect the desired intracellular delivery. We prepared a dimer of TATp as our model since it is the prototypical CPP that is widely studied to carry a variety of cargoes.[1, 4] Notably, there is a dearth in information about the use of multimeric TATp as carrier of covalently linked small molecule cargoes. Herein we describe the synthesis, orthogonal conjugation, and permeability characterization of a TATp dimer (TATp-D, **5**, Fig. 1) to HeLa and rat primary hippocampal neuronal cells.

Compound	Name	Sequence
1	KLA	X-KLALKALKAALKLA-NH_2
2	R_8	X-RRRRRRRR-NH_2
3	Penetratin	X-RQIKIWFQNRRMKWKK-NH_2
4	TATp	X-GRKKRRQRRRPPQ-NH_2
5	TATp-D	Ac-GRKKRRQRRRPPQ Ac-GRKKRRQRRRPPQ-K-K-NH_2
X= Fluorophore Cyanine 5 (Cy5)		X

Figure 1. Cell penetrating peptides investigated in this study.

Our multimerization approach utilizes a bis-Fmoc protected Lys as a branch point near the *C*-terminus (Scheme 1).[12] This approach allows for possible multiple branching that can be used to generate the desired multimer in a non-combinatorial fashion, maximizing synthetic efficiency and discretely controlling valency. This approach also leaves the originally described sequence unaltered and does not depend on the existence or addition of specific residues within a peptide sequence, such as a previous report on dimeric variant of the CPP called sC18 that branched out from the Lys residue within the CPP.[9] This strategy also led to a divalent CPP

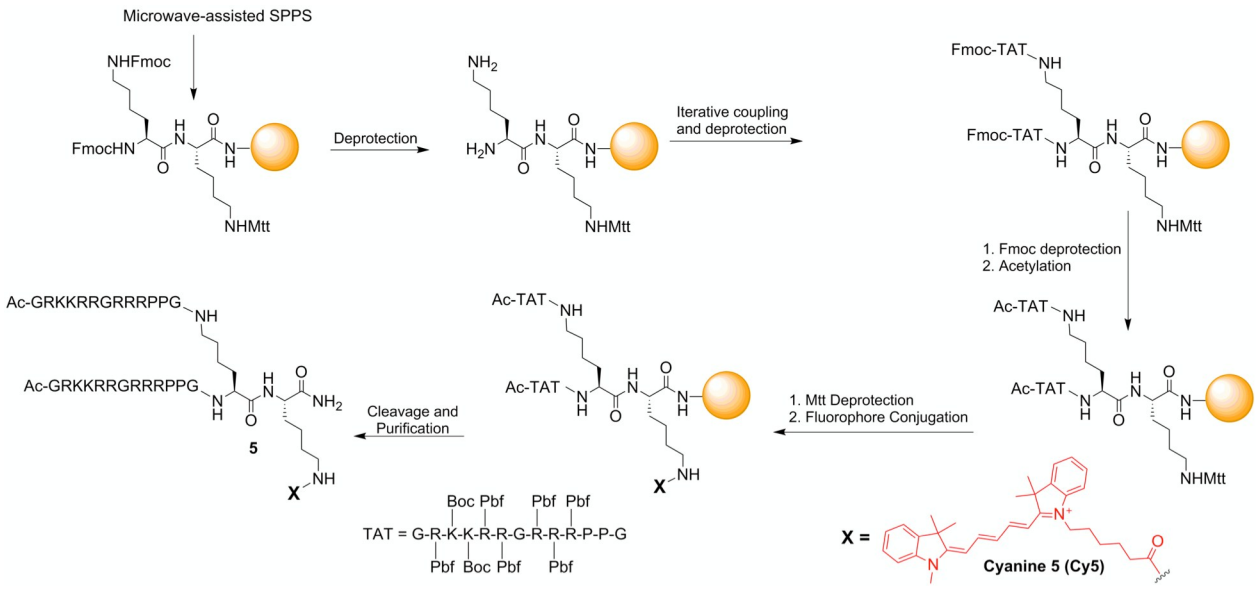

Scheme 1. Synthetic route for the preparation of branched dimeric Tat peptide (TATp-D, **4**) by microwave-assisted solid phase peptide synthesis.

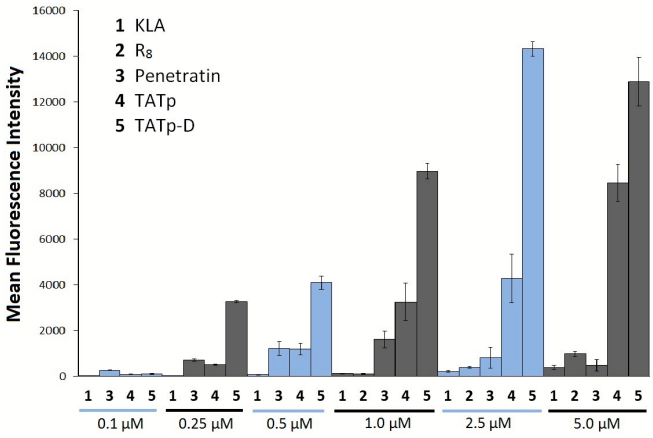

Figure 2. Membrane permeability to HeLa cells by flow cytometry. (a) Mean fluorescence intensity (MFI) of HeLa cells indicating that TATp-D (**5**) is very permeable *vs* other tested CPPs at 0.25-2.5 μM.

without the need for complicated native chemical ligation or disulfide bond formation that may lead to uncontrolled multimerization and non-homogenous mixture of species that make reproducibility of synthesis and characterization difficult. While control of multivalency is crucial, it is also necessary to generate a delivery agent that is easily conjugated with desired cargoes in a controlled manner. This orthogonally-protected design offers a control to selectively conjugate different cargoes at either or both termini after solid phase synthesis. We achieved this by utilizing the orthogonally- protected ε-4-methyltrityl (Mtt) protected Lys residue at the *C*-terminus. Mtt is an acid sensitive protecting group that could be removed under mildly acidic conditions (1-2% TFA, Scheme 1),[13] allowing the selective on-resin attachment of a desired cargo at this position post synthesis via an amide linkage. Meanwhile, the *N*-terminal Fmoc can be removed and directly conjugated with a different cargo prior to peptide cleavage or can be tagged with maleimide for post cleavage conjugation of a cargo via Michael addition.

The cell penetrating peptides investigated in this study were prepared by microwave-assisted solid phase synthesis using either Initiator$^+$ SP Wave or Alstra from Biotage. During the synthesis of TATp (**4**), we identified inefficient coupling steps at locations with sequential Arg residues, possibly because of the sterics imparted by Arg side chain and Pbf-protected guanidino moiety (Supplementary information). Prompted by these observations, we performed double or triple couplings at these critical positions to ensure the efficient growth of the peptides on the solid support. Acetyl groups were appended to TATp-D (**5**) as model cargo at the *N*-termini. The peptides were then labeled with the fluorophore Cyanine5-CO_2H (Cy5) (represented by X in Fig. 1 and Scheme 1) to serve as reporter molecule and surrogate biomolecule cargo. The peptides were cleaved using TFA/TIS/H_2O, purified by reversed phase HPLC using Waters XBridge C_{18} column, and lyophilized to yield fluffy blue powder of the TFA salt of the peptides. The peptides were then converted to chloride salts prior to use in all cell-based assays.[14]

Initial peptide uptake was evaluated using human epithelioid cervical carcinoma (HeLa) cells by measuring cell fluorescence intensity via flow cytometry. HeLa cells were chosen because it is one of the widely used models in cell penetration assays.[4] The cells were treated with 100 nM to 5.0 μM TATp-D (**5**) and incubated for 1 h at 37 °C. Uptake efficiency was compared to octaarginine (R_8, **2**), penetratin (**3**), and TATp (**4**) as positive controls and to a non-permeable scrambled form of KLA (**1**) as a negative control.[15] Mean fluorescence intensities (MFI) were averaged over three gated values using a range of 3,000 to 10,000 cells per treatment and normalized to TATp (**4**). Interestingly, peptide **5** showed enhanced uptake compared to **4** across all tested concentrations (Fig. 2). Furthermore, at 0.25 to 2.5 μM, the membrane permeation property of **5** was significantly higher than that of **2**, **3**, and **4**, and was not linearly correlated with the number of TATp units in **5** or concentration (Fig. S8). The greatest uptake of **5** relative to other CPPs at the same concentration was observed at 0.25 μM (Fig. 2a), i.e. HeLa cells treated with 0.25 μM **5** showed comparable fluorescence intensity as those cells treated with 2.5 μM of **4**, reflecting an order of magnitude increase in permeability (Fig. 2). These findings support the hypothesis that multivalency can dramatically increase the potency of a CPP. Further, these observations suggest that the current design may have built a synergistically enhanced ability to cross the plasma membrane due to increased local concentration on the membrane surface, the exact origin of which remains to be elucidated. We

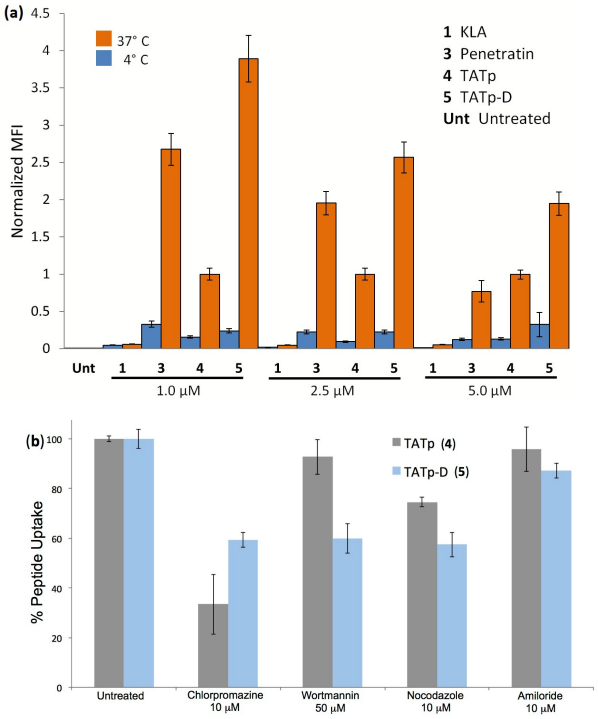

Figure 3. Mechanism of Entry Studies using HeLa cells. (a) Uptake of TATp (**4**) and TATp-D (**5**) are reduced at 4 °C as compared to 37 °C, indicating energy dependent entry of both peptides. (b) Effects of endocytosis inhibitors on the uptake of **4** and **5**. Error represented as SD, n=3.

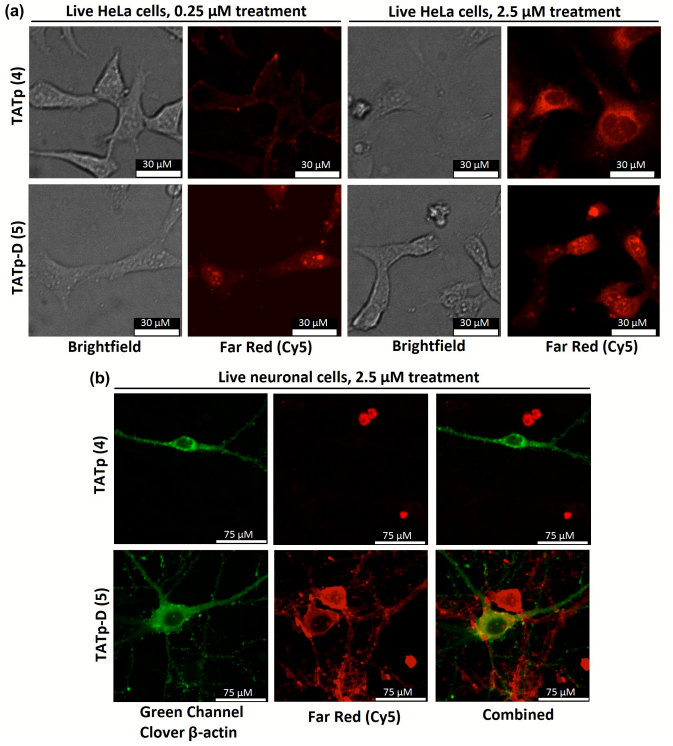

Figure 4. Confocal microscopy images taken at 20x magnification. (a) HeLa cells; (b) Primary hippocampal neuronal cells. Live cell images taken following 30 min incubation at 37 °C in imaging buffer.

speculate that part of this enhancement is due to increased interaction between **5** and the cell membrane, specifically through amplified guanidinium-phospholipid interactions.[16]

To investigate if dimerization has altered the known energy dependent membrane permeation mechanism of TATp (**4**) at these concentrations, we performed parallel flow cytometry assays after incubating HeLa cells at 37 and 4 °C. The mean fluorescence intensity (MFI) values were normalized to **4** at 37 °C to enable a direct comparison of observed fluorescence intensities. HeLa cells treated with **3**, **4** or **5** and incubated at 4 °C showed a drastic decrease in fluorescence (Figure 3a). This suggests that although **5** shows enhanced uptake, its membrane permeation mechanism may not deviate from the known energy dependent uptake of **4**.[16, 17]

We sought to determine the mechanism of cell entry of **5** using endocytosis inhibitors following known strategies that elucidated the mechanism of entry of TATp.[17, 18] Chlorpromazine, wortmannin, nocodazole, and amiloride were chosen as probes of clathrin-mediated endocytosis, macropinocytosis via phosphatidylinositol-3-kinase, caveolae-mediated endocytosis, and macropinocytosis via sodium-proton exchange, respectively.[17, 18] Peptide uptake was normalized to peptide-treated HeLa cells without inhibitor. Chlorpromazine showed the highest inhibition of **4**, causing 67% reduction in uptake (Fig. 3b) that is consistent with prior reports that clathrin-mediated endocytosis is a major pathway of TATp entry.[4] TATp-D (**5**) is sensitive to wortmannin, nocodazole, and chlorpromazine that led to 50, 43, and 40% reduction in peptide uptake, respectively, suggesting that **5** may have stimulated multiple mediators of the entry process. Both peptides were unaffected by amiloride. Additionally, since the guanidinium moiety of Arg residues is believed to form up to five hydrogen bonds with membrane lipid phosphates,[16] the increased local concentration of TATp via multimerization may have contributed to a favorable interaction that led to stimulation of multiple modes of uptake.[16, 19] Although more rigorous investigations are needed to understand these observations, it is possible that the increased kinetics and uptake efficiency of **5** is mediated by the synergistic effects of simultaneous activation of these pathways. We also evaluated the toxicity of the peptides to HeLa cells using the 3-(4,5-dimethyl-2-thiazolyl)-2,5-diphenyl-2H-tetrazoliumbromide (MTT) assay and found that 5 is not cytotoxic even up to 50 µM (Fig. S11). We also evaluated membrane integrity via a lactate dehydrogenase leakage (LDH) assay ultimately finding no significant membrane disruption up to 50 µM (Fig. S12), ten-times the highest tested concentration in our membrane permeability assay.

We performed confocal laser scanning microscopy to visually evaluate cellular uptake of TATp (**4**) and TATp-D (**5**) using HeLa and primary neuronal hippocampal cells. Live cell imaging of HeLa cells was performed at 37 °C using **4** and **5** at 0.25 and 2.5 µM peptide concentrations, with images taken at identical instrument settings at each chosen peptide concentration treatment. Immediately after peptide treatment, images were taken every 30 s at the far red (640 nm) channel for a total of 30 min. The images were compiled to constitute a time-lapse video of the peptides crossing the plasma membrane (Supplementary videos). As the images show in Fig. 4a, peptide **5** is evidently more permeable than **4** on HeLa cells at 0.25 µM, localizing in the cytoplasmic region while **4** appears to minimally enter the cells and is mostly localized around the cell periphery. This difference is also evident at 2.5 µM where **4** permeated the cell, but appeared more punctate and apparently nuclear excluded as compared to **5**. The videos also show dramatic differences in membrane permeation and intracellular concentration of the peptides. HeLa cells treated with **5** at 0.25 µM turned brilliant red throughout the intracellular region within 1 min, while those treated with **4** at 0.25 µM were not very fluorescent even after a 30 min incubation (Supplementary videos). By measuring the

fluorescence intensity of the cytoplasm of HeLa cells, we found that **5** at 0.25 μM has comparable translocation efficiency as **4** at 2.5 μM (Fig. S15), corroborating our flow cytometry observations. Aside from overall enhanced uptake, **5** also showed faster cell entry kinetics, a valuable characteristic for overcoming the typical short in vivo half-life of protein-derived CPPs.[20]

We proceeded by treating the cells with 4% paraformaldehyde (PFA) and mounting on glass slides to generate fixed cell images. HeLa cells treated with **4** showed an altered peptide distribution as compared to those recorded for live cells, whereby nuclear localization and a more punctate distribution within the cytosol have become more pronounced (Fig. S14). Meanwhile, cells treated with **5** do not appear significantly altered. This reinforces the need to be cautious when interpreting uptake data for CPPs using fixed cell confocal microscopy as a tool.[21]

To test TATp-D (**5**) in cells that are more challenging to penetrate, we used primary neuronal cells from rat brains as models. These cells were pre-transfected with clover β-actin that allowed visualization of select neurons via green fluorescence.[22] Immediately after treatment with 2.5 μM of peptides **4** and **5**, images were recorded at both the green (488 nm) and far red (660 nm) channels as described above for HeLa cells. We found that **4** does not show very detectable uptake, requiring a longer exposure time ~60 ms to distinguish the cells from background signal (Fig. 4b and Supplementary videos). Meanwhile, peptide **5** permeated the clover β-actin transfected neurons as well as the surrounding glial cells as recorded at exposure times of 3-5 ms. (Fig. 4b and Supplementary videos). These findings further demonstrate that a simple multivalent design can dramatically improve the membrane permeation of a CPP to cells that are difficult to penetrate, such as primary brain cells. In fact, TATp has been shown to successfully deliver cargo to astrocytes but not to neuronal cells,[23] suggesting that engineering a simple multimeric CPP design like **5** may have built a synergistically enhanced ability to penetrate neurons. Our findings provide a precise account on demonstrating a simple, orthogonally functionalizable dimeric CPP that penetrates primary brain cells. As previously observed with HeLa cells, the fixation process perturbed the distribution of **4** and **5** in neurons (Fig. S14), thus corroborating the notion that fixed cell images of peptide-treated cells could give false-positive membrane permeability of uncharacterized CPP designs.

This work demonstrates the utility of multimerization and represents a simple approach to multivalent CPPs that show great promise in improving existing CPP technologies. TATp-D (**5**) showed a six- to seven-fold fluorescence increase versus TATp (**4**) at 0.25 μM. TATp-D also translocated in neuronal cells with no apparent increase in cytotoxicity. This orthogonally protected design enabled the selective conjugation of different cargoes at the *N*- and *C*-termini, on- or off-resin. Furthermore, our results suggest that the method presented herein is applicable for the preparation of higher valency CPPs to improve their membrane permeability at lower concentrations, which is beneficial in the delivery of high-value therapeutics. In the future, we will determine if TATp-D decorated with two different cytotoxic cargoes at the *N*- and *C*-termini will show enhanced efficacy against a panel of cancer cell lines. We will also perform co-localization studies to determine if the peptide distributes in the cytoplasm and the nucleus.

This work was supported by Washington State University Startup Fund, Biotage Corp., and Waters Corporation New Faculty Grant for JPS. HCA acknowledges the support from NIH/NIAID (R01AI109022). GAW acknowledges the support from NIH (MH086032). We acknowledge the support of Dr. N. Lewis (WSU Inst. for Biological Chemistry) by providing access to Waters Synapt G2 MALDI-TOF-MS funded by NSF (DBI-1229749).

Notes and references

[1]Department of Chemistry, [2]Paul G. Allen School for Global Animal Health, [3]Department of Neuroscience, and [4]Institute for Biological Chemistry, Washington State University, Pullman, Washington 99164, U.S.A.
Email: jonel.saludes@wsu.edu; Online: www.saludeslab.org
Tel: +1-509-335-1144; Fax: +1-509-335-8867

† Electronic Supplementary Information (ESI) available: [Experimental details, MS, flow cytometry, cell viability, membrane integrity, confocal microscopy data]. See DOI: 10.1039/c000000x/

1 E. G. Stanzl, B. M. Trantow, J. R. Vargas and P. A. Wender, *Acc. Chem. Res.*, 2013, **46**, 2944.
2 C. Bechara and S. Sagan, *FEBS Lett.*, 2013, **587**, 1693.
3 A. D. Frankel and C. O. Pabo, *Cell*, 1988, **55**, 1189.
4 D. M. Copolovici, K. Langel, E. Eriste and U. Langel, *ACS Nano*, 2014, **8**, 1972.
5 S. Futaki, *Adv. Drug Delivery Rev.*, 2005, **57**, 547.
6 K. Kamide, H. Nakakubo, S. Uno and A. Fukamizu, *Intl. J. Mol. Med.*, 2010, **25**, 41.
7 W. L. Zhu and S. Y. Shin, *J. Pept. Sci.*, 2009, **15**, 345; F. S. Hassane, G. D. Ivanova, E. Bolewska-Pedyczak, R. Abes, A. A. Arzumanov, M. J. Gait, B. Lebleu and J. Gariepy, *Bioconj. Chem.*, 2009, **20**, 1523; A. M. Angeles-Boza, A. Erazo-Oliveras, Y. J. Lee and J. P. Pellois, *Bioconj. Chem.*, 2010, **21**, 2164; G. A. Eggimann, S. Buschor, T. Darbre and J. L. Reymond, *Org. Biomol. Chem.*, 2013, **11**, 6717; G. A. Eggimann, E. Blattes, S. Buschor, R. Biswas, S. M. Kammer, T. Darbre and J. L. Reymond, *Chem. Commun.*, 2014, **50**, 7254.
8 S. H. Park, J. Doh, S. I. Park, J. Y. Lim, S. M. Kim, J. I. Youn, H. T. Jin, S. H. Seo, M. Y. Song, S. Y. Sung, M. Kim, S. J. Hwang, J. M. Choi, S. K. Lee, H. Y. Lee, C. L. Lim, Y. J. Chung, D. Yang, H. N. Kim, Z. H. Lee, K. Y. Choi, S. S. Jeun and Y. C. Sung, *Gene Ther.*, 2010, **17**, 1052.
9 J. Hoyer, U. Schatzschneider, M. Schulz-Siegmund and I. Neundorf, *Beilstein J. Org. Chem.*, 2012, **8**, 1788.
10 P. Sommer, V. S. Fluxa, T. Darbre and J. L. Reymond, *ChemBioChem*, 2009, **10**, 1527.
11 A. Kwok, G. A. Eggimann, J. L. Reymond, T. Darbre and F. Hollfelder, *ACS Nano*, 2013, **7**, 4668.
12 W. L. Zhu and S. Y. Shin, *J. Pept. Sci.*, 2009, **15**, 345.
13 D. Li and D. L. Elbert, *J. Pept. Res.*, 2002, **60**, 300; J. P. Saludes, L. A. Morton, S. K. Coulup, Z. Fiorini, B. M. Cook, L. Beninson, E. R. Chapman, M. Fleshner and H. Yin, *Mol. BioSyst.*, 2013, **9**, 2005.
14 V. V. Andrushchenko, H. J. Vogel and E. J. Prenner, *J. Pept. Sci.*, 2007, **13**, 37.
15 A. Scheller, B. Wiesner, M. Melzig, M. Bienert and J. Oehlke, *Eur. J. Biochem.*, 2000, **267**, 6043.
16 Y. C. Su, T. Doherty, A. J. Waring, P. Puchala and M. Hong, *Biochemistry*, 2009, **48**, 4587; Y. Su, A. J. Waring, P. Ruchala and M. Hong, *Biochemistry*, 2010, **49**, 6009.
17 F. Madani, S. Lindberg, U. Langel, S. Futaki and A. Graslund, *J. Biophys.* 2011, **2011**, 414729.
18 S. Al-Taei, N. A. Penning, J. C. Simpson, S. Futaki, T. Takeuchi, I. Nakase and A. T. Jones, *Bioconj. Chem.*, 2006, **17**, 90; E. Vives, P. Brodin and B. Lebleu, *J. Biol. Chem.*, 1997, **272**, 16010; S. B. Sieczkarski and G. R. Whittaker, *J. Gen. Virol.*, 2002, **83**, 1535.
19 S. H. White and W. C. Wimley, *Ann. Rev. Biophys. Biomol. Struct.*, 1999, **28**, 319.
20 M. Fotin-Mleczek, S. Voss and R. Brock, in *Handbook of Cell Penetrating Peptides*, Ed: U. Langel, Taylor & Francis, Boca Raton, FL, 2007, pp. 161-182.
21 M. Lindgren, M. Pooga and U. Langel, in *Handbook of Cell Penetrating Peptides*, Ed: U. Langel, Taylor & Francis, Boca Raton, FL, 2007, pp. 567-587.
22 M. Dhar, G. A. Wayman, M. Zhu, T. J. Lambert, M. A. Davare and S. M. Appleyard, *J. Neurosci,*, 2014, **34**, 10022; G. A. Wayman, Y.-S. Lee, H. Tokumitsu, A. Silva and T. R. Soderling, *Neuron*, **59**, 914.
23 M. J. Simon, S. Gao, W. H. Kang, S. Banta and B. Morrison, *Biotechnol. Bioeng.*, 2009, **104**, 10.

